

Fig. 3. Particle size-velocity correlation coefficient

cases, the correlation coefficient varies across the jet because of the statistical errors associated with the averaging technique.

In conclusion, I have presented a set of data that quantify the errors associated with velocity bias in the measurement of

the first two moments of the velocity field and those associated with the measurement of the velocity-particle size correlations. Furthermore, the errors are in the range of 10–15% for the measurement of the Reynolds stress and 20–30% for measurement of the third moments. Despite the similarity in seeding, the velocity field is not uniformly correlated to the particle dynamics when arithmetic or 1-D averaging is used as compared to residence time weighting.

References

1. Adrian RJ (1983) Laser velocimetry. In: Fluid mechanics measurements (ed. R.J. Goldstein), Hemisphere Publishing Corporation
2. Capp SP (1983) Experimental investigation of the turbulent axisymmetric jet. Phd thesis University at Buffalo, SUNY
3. George WK (1988) Quantitative measurement with the burst-mode laser Doppler anemometer. *Experimental thermal and fluid science* 1: 29–40
4. Hussein HJ; Capp S; George WK (1994) Velocity measurements in a high-Reynolds-number, momentum-conserving, axisymmetric, turbulent jet. *J Fluid Mech* 258: 31–75
5. Hussein HJ; Stone JW; Arik BE (1991) Liquid-droplet interactions in an atomizing turbulent jet. AIAA Paper no. 91-0318
6. McLaughlin DK; Tiederman WG (1973) Biasing correction for individual realization laser anemometer measurement in turbulent flows. *Physics of Fluids* 16: 2082–2088
7. Stone JW (1990) A study of spray nozzle atomization by phase Doppler techniques. MS Thesis, Vanderbilt University

Reynolds number effect on the skin friction in separated flows behind a backward-facing step

S. Jovic, D. Driver

Experimental skin-friction measurements for different Reynolds number flows over a backward-facing step are reported. The Laser-Oil Flow Interferometry technique (LOI)

was used to measure the shear stress at the wall. This relatively new technique has proved to be more robust than conventional methods and does not depend on the law-of-the-wall. The technique provides a direct measurement of wall shear stress and is suitable and applicable in many complex flow configurations, including cases with massive separation where conventional techniques are likely to fail.

Present measurements reveal that the skin-friction coefficient magnitude decreases everywhere in the flow as the Reynolds number ($Re_h = U_0 h / \nu$) increases (U_0 is the reference velocity upstream of the step, h is the step height, and ν is the kinematic viscosity). This trend occurs both inside the recirculating zone as well as downstream in the recovery region. Furthermore, the local minimum skin-friction coefficient measured inside of the recirculating zone, $C_{f, \min}$, varies as $Re_h^{-1/2}$ for the range of Reynolds numbers tested. This finding suggests that the flow near the wall in the recirculating region is a viscous-dominated, laminar-like flow. The data

Received: 7 February 1994/Accepted: 30 August 1994

S. Jovic¹
Eloret Institute,
3788 Fabian Way,
Palo Alto, CA 94303, USA

D. Driver
NASA Ames Research Center, MS 229-1, Moffett Field,
CA 94035-1000, USA

Correspondence to: D. Driver

¹Mailing address: NASA Ames Research Center, MS 229-1,
Moffett Field, CA 94035-1000, USA

Research support for the first author was provided by NASA Grant NCC2-465, and is gratefully acknowledged.

further demonstrate that the use of “Clauser chart” or Preston tubes will yield grossly inaccurate estimates of shear stress in the reattached and recovering flow region particularly for lower Reynolds numbers.

1

Introduction

This experimental investigation was inspired by the need to validate a Direct Numerical Simulation (DNS) of a backstep flow being carried out by the Joint Stanford/NASA Center for Turbulence Research (Le, Moin and Kim 1993).

A backward-facing step configuration was chosen because of its relatively simple geometry, which facilitates both the experiment and computations.

Previous experiments on backstep flows were typically performed at significantly higher Reynolds numbers than the DNS could hope to duplicate due to limited computer speed and storage needed to resolve the small time and length scales of high Reynolds number turbulence. Those experiments whose Reynolds numbers are sufficiently low do not contain flowfield data. The DNS calculations in the present case were performed at a $Re_h = 5100$ with the boundary layer thickness $\delta = h$ (upstream of the step) and the expansion ratio, $E_r = 1.2$ (E_r is the ratio of the tunnel areas immediately downstream and upstream of the step). The Reynolds number of the upstream boundary layer, based on the momentum thickness, was $Re_\theta = 600$. Previous experiments performed at higher Reynolds numbers produced significantly different results compared to those of the DNS. Therefore, the present experimental effort began with a study of Reynolds number effects.

The results of the Reynolds number effect study lead to the construction of a much smaller dedicated wind tunnel (10 cm \times 30 cm) which approximately matched the given parameters of the DNS. Complete results for that experiment are reported in a NASA Technical Memorandum (Jovic and Driver 1994).

The primary objective of this investigation was to study the influence of Reynolds number, Re_h , on the skin-friction distribution in three characteristic regions of a separated flow: the recirculating, the reattaching, and the recovering regions. In addition, the relationship between the minimum skin-friction coefficient, $C_{f, \min}$, in the recirculating flow region and the Reynolds number, Re_h , was also analyzed.

2

Experimental setup and conditions

Most of the experiments (cases 2 through 6 in Table 1) were conducted in an open-ended, low-speed wind tunnel facility whose cross-sectional area was 20 cm \times 42 cm. A zero pressure gradient section (169 cm long) upstream of the step produced boundary layers whose thickness ranged between 30 mm and 38 mm (depending on the tunnel speed). The boundary layer was tripped just downstream of the inlet contraction with a 1.6 mm diameter wire followed by a 110 mm length of 40 grit emery paper. The step height was varied by changing a series of filler blocks on the step-side wall of the wind tunnel. The minimum step height was 17 mm and the maximum was 38 mm. The ratio of boundary layer thickness to step height ranged from 0.79 to 2. The expansion ratio fell in the narrow range between 1.09 and 1.2. The aspect ratio (tunnel width to

Table 1. Summary of flow parameters

No.	Re_h	δ/h	Re_θ	U_0 (m/s)	h (mm)	E_r	x_r/h
1	5000	1.20	600	7.70	9.65	1.20	6.00
2	6800	2.00	1650	6.00	17.0	1.09	5.35
3	10400	1.27	1650	6.00	26.0	1.14	6.35
4	25500	1.20	3600	14.60	26.0	1.14	6.90
5	25500	0.82	2400	10.00	38.0	1.20	6.70
6	37200	0.82	3600	14.60	38.0	1.20	6.84
D&S	37500	1.50	5000	44.20	12.7	1.11	6.26

step height) varied from 11 for the largest to 24.7 for the smallest step. This aspect ratio is sufficiently large to ensure adequate two-dimensionality in the separated region, as has been demonstrated by deBrederod & Bradshaw (1972). The measurement domain extended 1940 mm downstream of the step.

An additional experiment (Jovic and Driver 1994) was conducted in a smaller wind tunnel whose cross-sectional area was 10 cm \times 30 cm. This tunnel contained a double sided expansion consisting of a 0.9 cm high step on both top and bottom walls of the wind tunnel. The pressure distribution associated with the double sided expansion is similar to the pressure distribution for the single sided expansion of the same expansion ratio. The double sided expansion was chosen to replicate the boundary conditions of the DNS which had a slip condition along its top boundary of the computational domain (i.e. experimental centerline).

Time-averaged skin-friction measurements were made using the Laser-Oil Interferometer technique described by Monson, Driver and Szodrach (1981), and Monson and Higuchi (1981). The basic principle of the techniques are as follows. A drop of oil on the tunnel floor thins due to the shear stress. A fraction of the incoming laser beam will reflect from the top surface of the oil, while the rest of the passing beam will reflect from the surface on which the oil sits. Both portions of the reflecting beam interfere with each other, constructively when the beam's path length (down and back) through the oil is an integer number of light wavelengths thick. Destructive interference occurs when the light path is a fractional number of wavelengths thick. The reflected light intensity of the two interfering beams is recorded by a photodiode that produces a time record of the change in oil thickness to which lubrication theory is applied to relate the wall shear (τ_w) to the oil thinning rate. The skin-friction coefficient is defined as

$$C_f = \frac{2\tau_w}{\rho \cdot U_0^2}$$

Assessed uncertainties of skin friction were $\pm 8\%$ in the recovery region and $\pm 15\%$ in the separated region for a $\pm 95\%$ confidence level (where the error percentage is relative to the locally measured C_f). The distribution of the skin-friction coefficient versus x/h was measured for six different Reynolds numbers, as summarized in Table 1. The data of the Driver and Seegmiller (1985) (referred to as D&S) experiment are also included in the Table 1.

Reynolds number, Re_h , was varied by changing the reference velocity, U_0 , and the step height, h . The boundary layer

thickness upstream of the step was a weak function of tunnel speed and was nearly constant over the range of operating conditions. The parameter δ/h varied mainly due to the variation of the step height.

Reattachment length, x_r , and expansion ratio, E_r , are also included in the table. The expansion ratio is a measure of the adverse pressure gradient acting on the separated free shear layer and of the favorable pressure gradient acting on the reversed flow in the recirculating region. Boundary layers upstream of the step were fully developed turbulent boundary layers. Reattachment length was determined from oil flow visualizations and errors in reattachment length were estimated to be less than ± 5 mm. All skin-friction and velocity measurements were made along the tunnel centerline.

The main test cases were 1 through 6 (see Table 1), however, additional experiments were performed with different Reynolds numbers in order to assess a relationship $C_{f, \min}$ vs. Re_h . Supplement measurements $C_{f, \min}$ were made in the 10 cm \times 30 cm tunnel for $Re_h = 6000, 8080, 10000, 12300$ and in the 20 cm \times 42 cm tunnel for $Re_h = 10500, 12000, 12700, 18000, 20000, 26000, 32000$.

3

Results and discussion

Skin-friction coefficient distributions for seven cases are presented in Fig. 1. It is seen that the skin-friction magnitude decreases with increasing Reynolds number, for the range of Reynolds numbers studied. The minimum skin-friction coefficient, $C_{f, \min}$, occurs at approximately $2/3x_r$ and its variation with Re_h is shown in Fig. 2. It is clearly seen that $C_{f, \min}$ increases as Re_h decreases. The solid line in Fig. 2 has a slope of $-1/2$, which suggests that the flow near the wall in the recirculating region is viscous-dominated or laminar-like, as argued by Adams, Johnston and Eaton (1984), Casto and Haque (1987), and Devenport and Sutton (1991).

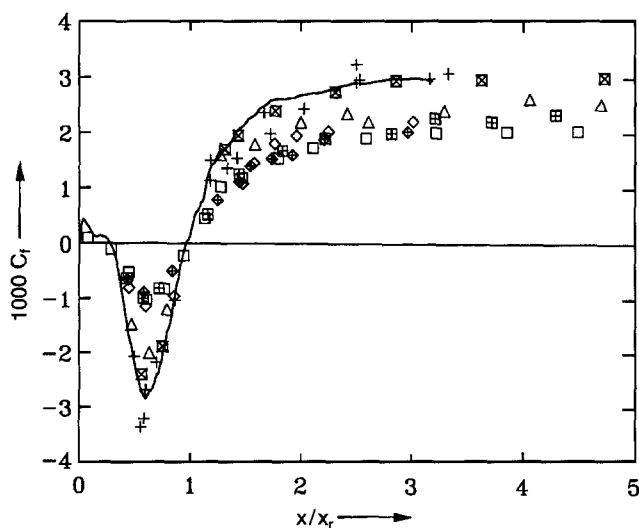


Fig. 1. Skin-friction coefficient distribution for different Re_h . Symbols: +, $Re_h = 5000$; \square , 6800; \triangle , 10400; \diamond , 25500; \diamond , 25500; \square , 37200; \square , 37500 (D&S); —, DNS prediction (Le et al. (1994)), $Re_h = 5100$

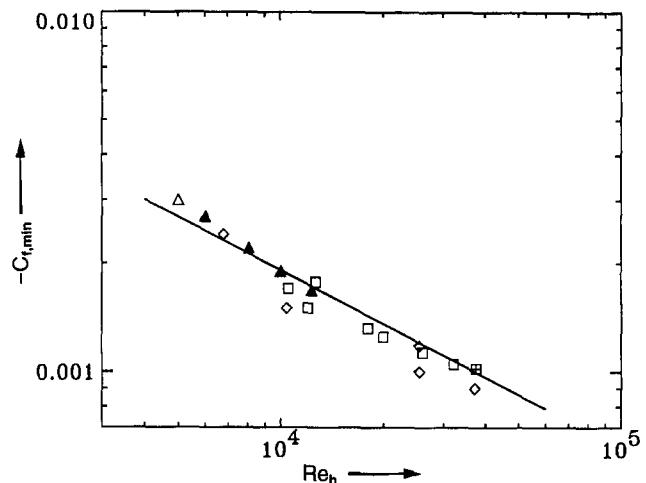


Fig. 2. $C_{f, \min}$ as a function of Re_h . Symbols: \triangle , measured in 10 cm \times 30 cm wind tunnel; \blacktriangle , other measurements in 10 cm \times 30 cm wind tunnel; \diamond , measured in 20 cm \times 42 cm wind tunnel (corresponds to rows 2 to 6 in Table 1); \square , other measurements in 20 cm \times 42 cm wind tunnel; \square , D&S; —, line with a $-1/2$ slope

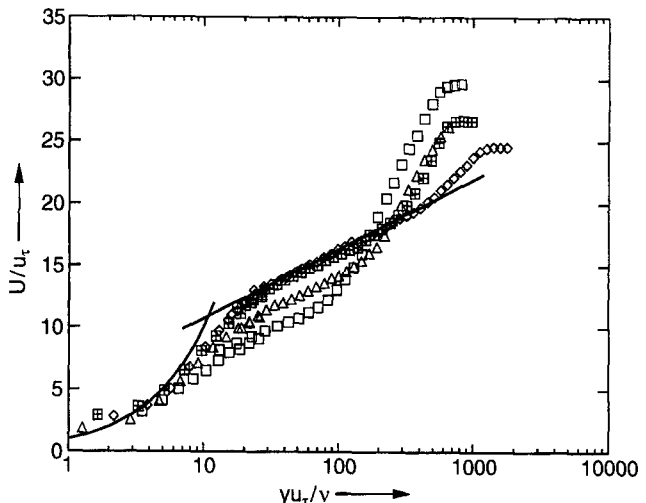


Fig. 3. Mean velocity distribution in wall coordinates normalized by the C_f measured by the LOI technique for $Re_h = 6800$. Symbols: \square , $x/h = 7.64$; \triangle , 12.35; \square , 25.29; \diamond , 114; —, linear and log-law velocity distribution.

Mean flow velocities were also measured in the region downstream of reattachment using a hot wire. Using $u_\tau = \sqrt{\tau_w / \rho}$ (obtained by the LOI method) for the normalization of the mean velocity, it became obvious that the mean flow does not scale with the standard log-law in the vicinity of the reattachment, as is seen in Fig. 3. Far downstream of reattachment the normalized mean velocity distribution does fall on the universal law-of-the-wall. It is apparent that using the Clauser method for deducing skin-friction will produce a low estimate for skin-friction. Also, skin-friction was deduced from a Preston tube (which also relies on the law-of-the-wall) and showed good agreement for $x/h > 25$, however, between $x_r < x < 25h$ the Preston tube gave systematically low values for C_f .

Conclusions

Results from the present study show that the skin-friction coefficient decreases as the Reynolds number, Re_h , increases in the following manner, $C_{f, \min} = -0.19 Re_h^{-1/2}$. The $-1/2$ power relationship deduced from the correlation $C_{f, \min}$ vs. Re_h indicates laminar like behavior which is consistent with the findings of Adams et al. (1984). Clauser's method, which is frequently used for the determination of the wall shear stress, leads to erroneous results when applied to the velocity measurements obtained in the near field of reattaching flows (and many other wall-bounded nonequilibrium flows). Direct measurements of the C_f using the LOI technique give higher values than those obtained by the classical techniques. The normalized mean velocity on the wall coordinates violates the universal law-of-the-wall in the near field of reattaching flows.

References

1. Adams EW; Johnston JP; Eaton JK (1984) Experiments on the structure of a turbulent reattaching shear layer. Rep. MD-43, Thermo-Sciences Div., Dept. Mech. Engng, Stanford University
2. deBredorod V; Bradshaw P (1972) Three-dimensional flow in nominally two-dimensional separation bubbles. I. Flow Behind a Rearward-Facing Step. I.C. Aero Report 72-19
3. Castro IP; Haque A (1987) The structure of a turbulent shear layer bounding a separation region: J Fluid Mech 179: 439
4. Davenport LW; Sutton EP (1991) Near-wall behavior of separated and reattaching flows. AIAA J 29: 25
5. Driver DM; Seegmiller HL (1985) Features of a reattaching turbulent shear layer in divergent channel flow. AIAA J 23: 163
6. Jovic S; Driver D (1994) Backward-facing step measurements at low Reynolds number. $Re_h = 5000$. NASA Technical Memorandum 108807
7. Le H; Moin P; Kim J (1993) Direct numerical simulation of turbulent flow over a backward-facing step. Report TF-58, Thermoscience Division, Department of Mechanical Engineering, Stanford University
8. Monson D; Driver D; Szodrich J (1981) Application of a laser interferometer skin-friction meter in complex flows. ICIASF '81 Record, International Congress on Instrumentation in Aerospace Simulation Facilities 232-243
9. Monson D; Higuchi H (1981) Skin friction measurements by a Dual-Laser-Beam Interferometer Technique. AIAA J 19: 739